PHASE GRADIENT APPROACH TO THE EVALUATION AND MAPPING OF GLACIER RHEOLOGY FROM MULTI-PASS SAR INTERFEROGRAMS

A.I. SHAROV, K. GUTJAHR
Institute of Digital Image Processing, Joanneum Research, Graz, Austria
E-mail: aleksey.sharov | karheinz.gutjahr@joanneum.at

P.E. PELLIKKA
Department of Geography, University of Helsinki, Finland
E-mail: petri.pellikka@helsinki.fi

Methodological design and technical performance of an original phase gradient approach to glacier rheological modelling and mapping will be discussed and several practical examples of utilising multi-pass ERS-1/2 SAR interferograms in different European glacial environments will be given.

1. Introduction

Evaluation and mapping of glacier rheology[1] is one of the most interesting and puzzling applications of differential radar interferometry (DINSAR). The DINSAR method based on differencing between two co-registered repeat-pass SAR interferograms of the same glacier provides a unique opportunity to detect and to measure even small glacier motions and ice deformations in the sub-centimetre range. Short-term ice velocities and their long-term variations can be surveyed with high spatial resolution over large glacial areas even if the glacier surface is snow-covered. Under favourable conditions, the accuracy of measuring the magnitude of ice-surface velocity from spaceborne differential interferograms is comparable with that from field surveys [1]. These unprecedented technical capabilities and notable availability of spaceborne interferometric data are greatly valued by experts studying glacier dynamics.

Numerous examples have already been shown of successful DINSAR applications to monitoring ice-sheet motion [2], mapping three-dimensional flow of large glaciers [3], measuring outlet glacier velocities [4], studying flow instability [5] and identifying surge effects on ice fields [6]. The performance of this generally promising technique is not always flawless, however, and there remains some uncertainty as to how it will operate in a given glacier environment and season different from those studied in preceding applications. In fact, previous applications of glacier interferometry were mostly *local* in character, each focussed on one or several neighbouring glaciers of the same morphological class, and only very few comparative studies have analysed the performance of the DINSAR method for different glacier types, extents and periods.

[1] Rheology is the branch of physics that studies the deformation and flow of matter [7].

Different methodological variants of DINSAR, such as 2-, 3-, 4- and multi-pass techniques, were exploited depending on the availability/quality of archival interferometric data and to a much lesser degree accounting for ice-flow peculiarities. Simplifying assumptions were frequently made, e.g. on the equality of glacier velocities at two different instants of time, to accelerate processing but turned out to be inappropriate for modelling a time-evolving glacier surface [8].

In the dynamic glacier environment, the applicability and accuracy of repeat-pass interferometry is strongly influenced by rapid physical changes of the ice surface and drastic temporal decorrelation of SAR signals between subsequent surveys performed at long intervals. Different temporal scales of interferometric and terrestrial surveys, the continuous albeit inhomogeneous character of ice flow and changeable glacier topography complicate the calibration and validation of DINSAR rheological models [9]. Other limitations to glacier interferometry are related to orbital data uncertainties, atmospheric influences, inaccuracies of reference topographic models (DEMs), algorithmic complexity and processing errors, mostly at the stage of interferometric phase unwrapping, detecting and resolving the line-of-sight motion, and geocoding.

The present paper reports on the design of an original and stringent albeit very simple algorithm for the reconstruction of glacier rheology from interferometric phase gradients (GINSAR) that does not involve complex process artifices, does not require accurate reference topographic models and provides fast, global and reliable solutions to:

- unsupervised detection of glacier motion/changes and distinguishing of areas with different degrees of ice deformation,
- quantitative evaluation and variational analysis of the glacier strain rate and ice velocities,
- representation of glacier rheology and morphology in the form of satellite *image maps*.

The GINSAR approach mitigates some problems related to the operation of interferometric phase unwrapping, thus improving modelling accuracy. Besides, fewer additional *a priori* assumptions have to be made on the character of glacier motion and glacier topography. The practical performance of this new method was tested using 7 pairs of repeat-pass ERS-1/2-SAR interferograms and numerous instrumental records documenting the rate of glacier ice flow in several test areas including Hintereisferner Glacier in the Austrian Alps, the Svartisen Ice Caps in Northern Norway and several large tidewater glaciers in the Western Russian Arctic.

2. Data and data gaps

14 repeat-pass ERS-1/2 INSAR tandem pairs taken at 1-day intervals under steady and cold weather conditions were selected for rheological studies and practical modelling of glacier dynamics in the Hintereisferner (HF), Svartisen (SV), and Western Russian Arctic (WeRA) test sites. The selection of INSAR pairs was performed so as to provide suitable spatial baselines within the range

of 0 – 200 m and to avoid unstable weather with high winds, heavy clouds, precipitation and melting at the glacier surface. The best interferograms for all test sites, with a typical mean coherence value of 0.68, were produced from SAR images taken during the cold season in October 1995 – April 1996. The lowest mean coherence value of about 0.47 was observed in an interferogram with a very short spatial baseline taken in the warm season. The main parameters of available INSAR data are specified in Table 1.

Table 1. List of the ERS-1/2-INSAR data obtained from ascending (A) and descending (D) orbits.

Date acquired E1/E2	Orbit E1/E2	Frame	$B_{\|\|}$, $B_{\perp}$ m	Weather
Hintereisferner Glacier				
10.01.96 / 11.01.96	23478 / 3805 A	0927	61, -163	Cs-As-St 4 / St 7
14.02.96 / 15.02.96	23979 / 4306 A	0927	-73, -135	St 5 / St 3, H
05.04.96 / 06.04.96	24709 / 5036 A	0927	51, 110	St 3 / St 8
Svartisen Ice Caps				
31.07.95 / 01.08.95	21138 / 1465 D	2259	-12, 0	Cu 3 / St 1, H
16.03.96 / 17.03.96	24416 / 4743 D	2259	14, 78	As - St 4 / Sc 1, H
28.03.96 / 29.03.96	24594 / 3242 A	1341	12, 10	Sc 1 / Sc 1, H
01.04.96 / 02.04.96	24645 / 4972 D	2259	-19, -56	Sc 2 / St – Sc 5
Western Russian Arctic (Franz Josef Land, Novaya Zemlya)				
03.09.95 / 04.09.95	21624 / 1951 D	1953	-19, -50	St-As 5 / St 4
08.10.95 / 09.10.95	22125 / 2452 D	1953	57, 129	Sc 3 / Sc 5
13.10.95 / 14.10.95	22201 / 2528 A	1557	10, 64	Sc 5 / St-Sc 7
05.03.96 / 06.03.96	24257 / 4584 D	2043	71, 165	St-As 5 / St 4, H
05.03.96 / 06.03.96	24257 / 4584 D	2061	69, 162	St-As 5 / St 4, H
18.03.96 / 19.03.96	24443 / 4770 D	2043	47, 155	St 3 / St 5, H
21.03.96 / 22.03.96	24486 / 4813 D	2061	13, -29	St 5 / St 5, H

All necessary Austrian, Norwegian and Russian topographic maps at scales ranging from 1:25 000 to 1:200 000 were also available. Besides, two raster digital elevation models (DEMs) with 25 m pixel size issued in the 1990s on the basis of topographic maps could be obtained for the SV and HF test sites. Preliminary tests, however, revealed a multitude of inaccuracies in those models with typical height errors of about ± 28 m and maximum errors exceeding 60 m. The topographic accuracy of the reference interferograms I_R synthesised from the DEMs was thus too low for their direct use in the conventional 2-pass DINSAR approach to the estimation of glacier motion.

Not many rheological maps have been published on the glaciers studied [10, 11], and it was rather difficult to find applicable reference data on ice flow in the test areas. There are very few instrumental records documenting the winter rate of ice flow and its spatial and seasonal variations in glacier accumulation areas. The average values of ice flow velocities, which were deduced from existing glaciological publications, did not exceed 0.1 m/day for Hintereisferner Glacier [12], 0.5 m/day for Engabreen Outlet Glacier in the SV test site [11] and 0.7 m/day for Shokal'skogo Glacier in the WeRA [13]. The same publications gave

some indications on the character of bedrock topography along the centreline of the test glaciers. Thanks to a remarkable stroke of good fortune we were able to borrow quantitative data on the annual 1995/96 and 1996/97 velocities of glacier flow in the lower half (3.5 km, 34 stakes) of Hintereisferner Glacier from the personal file of Mr. H.Schneider (University of Innsbruck) with kind permission of the proprietor.

In this study, we did not obtain precise absolute co-ordinates of ground control points, e.g. by special GPS measurements, but instead concentrated on measuring the relative parameters of glacier flow. The lack of basic ground-control data and insufficient quality of the rheological and topographic reference models - problems frequently encountered in glacier studies - were the principal reasons for applying the non-conventional GINSAR approach to modelling glacier dynamics in our test areas.

3. Methodological set-up

The idea of using SAR interferometric phase gradients for terrain modelling and studying related phenomena is not very new. 10 years ago, it was already demonstrated that phase gradient maps could be derived directly from complex SAR interferograms and applied to measuring both the magnitude and aspect of terrestrial slope without phase unwrapping [14, 15]. To our knowledge, the idea of applying the phase gradient approach to change detection was first presented in a paper by D.Sandwell and E.Price, who performed stacking and averaging of phase gradients with the aim of detecting and decreasing errors due to atmospheric-ionospheric disturbances in order to improve the general quality of INSAR data [16]. The subsequent work by our research group showed the applicability of this approach to the unsupervised detection of glacier changes and the spatial reconstruction of glacial flow from multi-pass INSAR data [17].

The underlying concept of the GINSAR approach is to proceed from operations on original SAR interferograms to the analysis of their derivatives, making use of the fact that, for the great majority of points in the interferential picture, partial gradients of the unwrapped interferometric phase $\Psi(x, y)$ are equal to partial gradients of the wrapped phase $\varphi(x, y)$, i.e.

$$\nabla\Psi_{x,y}(x,y) = \nabla\varphi_{x,y}(x,y),\ if\ \ \varphi(x,y) \in [-\pi,+\pi)\ ,\ \text{where}\ \ \Psi = \varphi + 2\pi k,\ k \in I\ . \quad (1)$$

In single-image processing, the value of gradient is assumed to be proportional to the difference in pixel values between adjacent pixels and, unlike [16], we calculate interferometric phase gradients by subtracting the original interferential picture from a shifted version of the same picture as *ortho-* or *cross-gradient:*

$$\overset{+}{\nabla}\varphi(x,y) = \nabla\varphi_x(x,y) + \nabla\varphi_y(x,y) \cong |\varphi(x+1,y) - \varphi(x,y)| + |\varphi(x,y+1) - \varphi(x,y)|\ ; \quad (2\,a)$$

$$\overset{\times}{\nabla}\varphi(x,y) \cong |\varphi(x+1,y+1) - \varphi(x,y)| + |\varphi(x,y+1) - \varphi(x+1,y)|\ . \quad (2\,b)$$

Considering the discrete character of the interferometric phase, partial gradients $\nabla\varphi_x$ and $\nabla\varphi_y$ can be directly converted to the relative height increments Δh_x and Δh_y by multiplying on the scaling factor $C(x,y)$, which depends on the imaging geometry, as

$$\Delta h_{x,y} \cong C(x,y)\cdot\nabla\varphi_{x,y} \quad \text{and} \quad C(x,y) = 0.25\pi^{-1}\cdot\lambda\cdot B_{\perp}^{-1}(x)\cdot R(y)\cdot\sin\theta(y)\ , \quad (3)$$

where $\lambda = 0.0566$ m is the wavelength of the SAR signal, $B_{\perp}$ *(x)* is the length of the perpendicular component of the baseline, *R(y)* - the slant range, *θ(y)* - the look angle.

The GINSAR image product specifying continuously the glacier height increments and providing a realistic view of the glacier surface is called a *topogram*. The topogram can be directly converted to a glacier *slope map* on a pixel-by-pixel basis using the algorithm offered in [17].

If the glacier topography is supposed to be unchanged between subsequent INSAR surveys, its contribution to the interferometric phase can be excluded by differencing between two co-registered multitemporal INSAR topograms of the same glacier. It is worth noting that, in contrast to combinatorial processing of original interferograms, each topogram can be scaled with any real, not necessarily integer factor, which makes further processing flexible and allows for any linear combination between multitemporal topograms. Assuming that $\nabla\varphi = \nabla\varphi_{topo} + \nabla\varphi_{mot}$ and $C_1\cdot\nabla\varphi_{topo\,1} = C_2\cdot\nabla\varphi_{topo\,2}$, the operation of differencing between two topograms can be formulated as follows

$$F = C_1\cdot\nabla\varphi_{mot\,1} - C_2\cdot\nabla\varphi_{mot\,2}\,. \quad (4)$$

The resultant picture *F(x,y)* containing only the differential motion phase without topographic phase is called *fluxogram* in reference to the name *fluxions* (from Latin fluxus – flow, continual change) that Isaac Newton gave to differential calculus. The fluxogram provides a very useful product that can be directly applied to the detection of glacier motion and to the delineation of moving areas. Moreover, the processing quality can be readily checked by controlling the representation of steady landforms in different parts of the fluxogram.

In order to solve the basic differential equation (4) with regard to the motion phase gradients $\nabla\varphi_{mot\,1}$ and/or $\nabla\varphi_{mot\,2}$, we assumed that the relation between ice-velocity gradients remains constant over the time span *ΔT* covered by both interferograms, i.e. $\nabla\varphi_{mot\,2} / \nabla\varphi_{mot\,1} = a$. This *steady flow assumption* seems to be more reliable in fast moving areas of the test glaciers than the constant velocity constraint. The *non-zero* reference values for $\nabla\varphi_{mot\,1}$ and $\nabla\varphi_{mot\,2}$ were determined for the limited number of characteristic points in two co-registered multitemporal topograms generated from the differential interferograms $I_1 - I_{R1}$ and $I_2 - I_{R2}$. The reference interferograms I_{R1} and I_{R2} without motion term

were synthesised from the available DEM. The limited accuracy of the simulated reference interferograms is not very critical in this case. Subsequently, the fluxogram was converted to a new image product using the following relation

$$\nabla \varphi_{mot\,1} = \Delta V_1 \cdot T_1 = F \cdot (C_1 - aC_2)^{-1}, \tag{5}$$

where ΔV_1 is the velocity gradient in the first interferogram.[2]

Such a scaled fluxogram also proves to be a desirable outcome of the GINSAR technique because it can be used for the analysis of the glacier strain rate, which is calculated as a difference between two neighbouring velocity values divided by the distance between velocity records.[3] A high value of the strain rate is an important indicator for the possible occurrence of crevasses on the glacier surface, which represent a serious hazard for hikers. During our field observations on Western Svartisen we revealed several *buried* crevasses near the ice divide; their location coincided with local maximum values of the strain rate in the GINSAR fluxogram. The fluxogram is usually averaged before calculating the strain rate.

Still, the image product described by equation (5) provides only relative information about the glacier velocity variations. In order to obtain absolute values of glacier velocity, the integration of motion phase gradients in the scaled fluxogram has yet to be performed. We perform such integration by applying the modification of the Cholesky algorithm to solving an over-determined system of linear equations, which relate the unknown velocities to their gradual observations in a least-square manner. In order to reduce the computational load, we perform this procedure only for the moving areas, which have been delineated in the fluxogram, thus excluding steady areas from the processing and diminishing areal error propagation. The product of integration representing the distribution of ice velocity over the glacier surface is called a *velogram*. The combination of several SAR topograms/fluxograms obtained from opposite, i.e. ascending and descending orbits, and/or the assumption of surface parallel flow allowed the ice-velocity component in the satellite look direction to be resolved into its horizontal and vertical constituents.

The GINSAR processing chain thus involves deterministic operations of calculating interferometric phase gradients from multi-pass interferograms, co-registering and differencing between scaled multitemporal topograms, thus eliminating the topographic phase term, and converting the differences obtained to the surface-motion field. A simplified flowchart showing the principal stages and main output products of the GINSAR approach is given in Figure 1.

In general, the interferometric scheme is much more sensitive to the surface motion than to the surface relief, and the rate of motion fringes in the interferential picture of an active glacier is usually much higher than that of

---

[2] Some reference values for the function *a(x,y)* can also be determined by analysing the frontal velocity gradients derived from winter interferograms of tidewater glaciers (I_3 in Fig. 1) on the basis of the transferential approach described in [17].

[3] Assuming that the direction of glacier flow coincides with the radar range direction.

topographic fringes. Hence, the differentiation procedure given by equations (2 a, b) partly or completely attenuates the topographic component and emphasises the motion phase. Local quantitative analysis of ice motion can, therefore, be performed even in *single* topograms. Figure 2 shows, for example, the cross-gradient image (b) obtained from the original 1-day interferogram (a) of 3/4 September 1995 ($B_{\perp}$ = - 50 m) in accordance with equation (2, b). In the gradient image, topographic fringes are completely removed, although extensive landforms with steep slopes and relief amplitude of more than 150 m are still detectable. Nevertheless, the system of secondary fringes (marked with **V**) can be seen within the area of rapid glacial flow on Simony Glacier and outlet glacier No.18 at McClintock Island in the Western Russian Arctic.

Similar features could be traced on almost all outlet glaciers in different gradient images of the study area. The visibility of secondary fringes depends on glacier orientation and can be enhanced by manipulating the shift value separately in azimuth and range direction. The width of secondary fringes reaches 500 meters and, although their rate decreases slightly in winter topograms, it remains very similar in different gradient images in spite of quite different spatial baselines. We therefore concluded that these features result from glacier movements and assumed that the relative velocity difference between two points on the glacier surface can be approximately determined in the radar line-of-sight direction by counting the number k of secondary fringes enclosed between those points as

$$\Delta V_{LOS} \cong 0.5\lambda \cdot k \cdot (T \cdot \cos\beta)^{-1}, \tag{6}$$

where β is the flow direction angle measured from the cross-track direction, and T = 1 day is the temporal baseline of the interferogram.

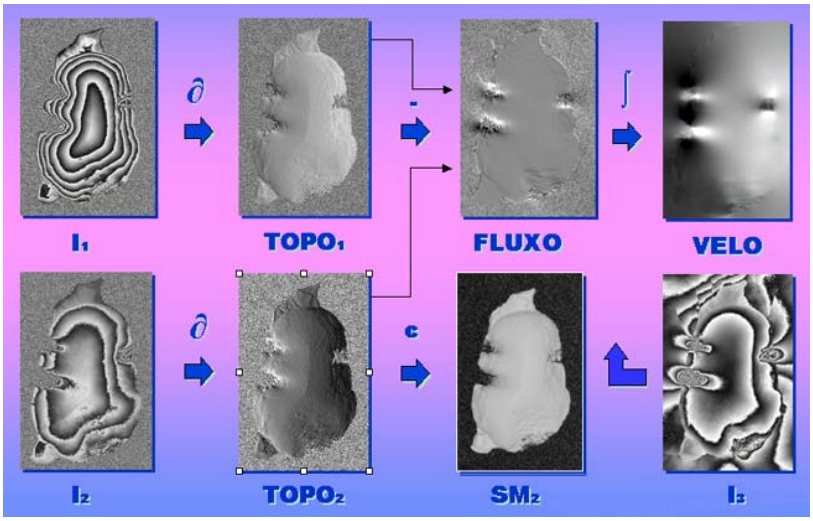

Figure 1. Principal stages of the GINSAR technique and GINSAR products of the Vostok-1 Ice Dome situated on La Ronciere Island, WeRA ($I_{1,2,3}$ – SAR interferograms, SM_2 - slope map).

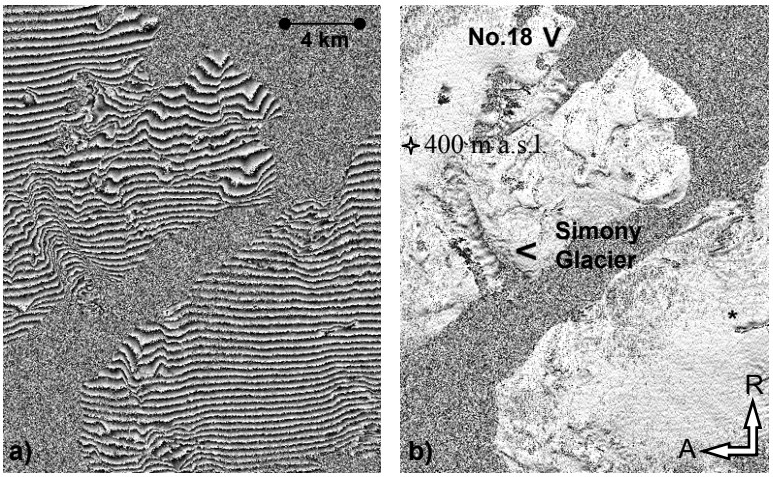

Figure 2. Original 1-day interferogram (a) and cross-gradient image (b) of Simony Tidewater Glacier, Western Russian Arctic. Secondary motion fringes are marked with **V**.

4. Main results

The INSAR pairs were processed using precise orbital data and a new release of the RSG 4.0 software package. All output GINSAR products were geocoded using available DEMs and represented in the form of an RGB image. The first two layers represent partial rheological quantities, e.g. partial velocity increments, defined separately in azimuth and range direction, and the third layer gives the full (absolute) value, e.g. the full velocity gradient, which is usually defined as an algebraic sum of partial quantities. In special applications, the conversion factor $C(x, y)$ can be presented as an additional fourth layer to the topogram, fluxogram or slope map. An example showing our GINSAR value-added products of Svartisen Ice Caps generated from two INSAR data sets of 16/17 March and 01/02 April 1996 is given in Figure 3. In this case, reference values for the ratio $\nabla\varphi_{mot\,2} / \nabla\varphi_{mot\,1}$ varied from 0.8 to 1.0 depending on the location.

A new cartographic concept including the layout, information contents, cartographic projection, symbols, legends, etc. was elaborated for producing *satellite image maps* of glacier rheology and changes. Several rheological maps showing glacier dynamics in the test sites at different scales ranging from 1:50 000 to 1:600 000 were compiled and published (Figure 4). The tachometric accuracy test for the rheological image map shown in Fig. 4 was carried out by comparing surface velocities at 11 tie points[4] identified in both the GINSAR image map sheet and the existing map substitutes based on photogrammetric surveys of ice velocities published in [11]. The results of accuracy tests are

[4] Tie points are those of known elevation and velocity.

summarised in Table 2. The mean difference between photogrammetric and GINSAR velocities was – 0.5 cm/day and the r.m.s. difference ± 2.25 cm/day.

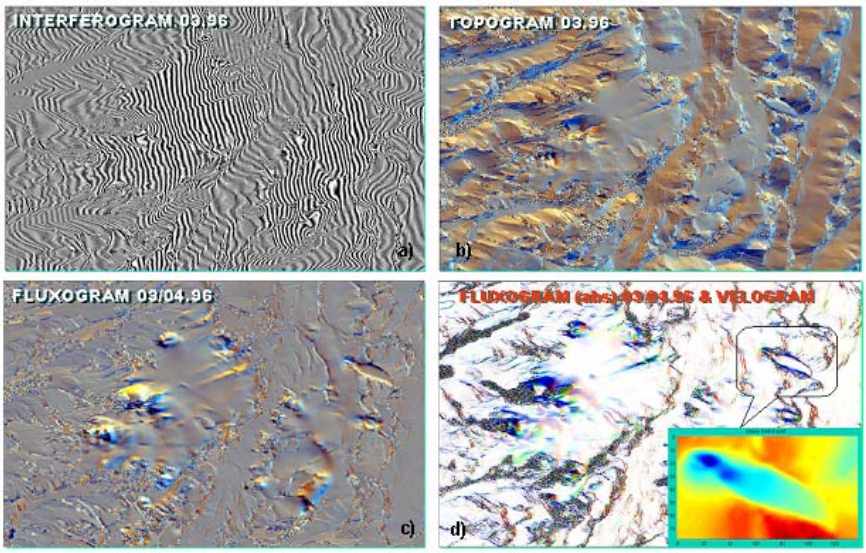

Figure 3. GINSAR products of Svartisen Ice Caps: original interferogram (a), topogram (b), fluxogram (c), fluxogram (module) and velogram (d).

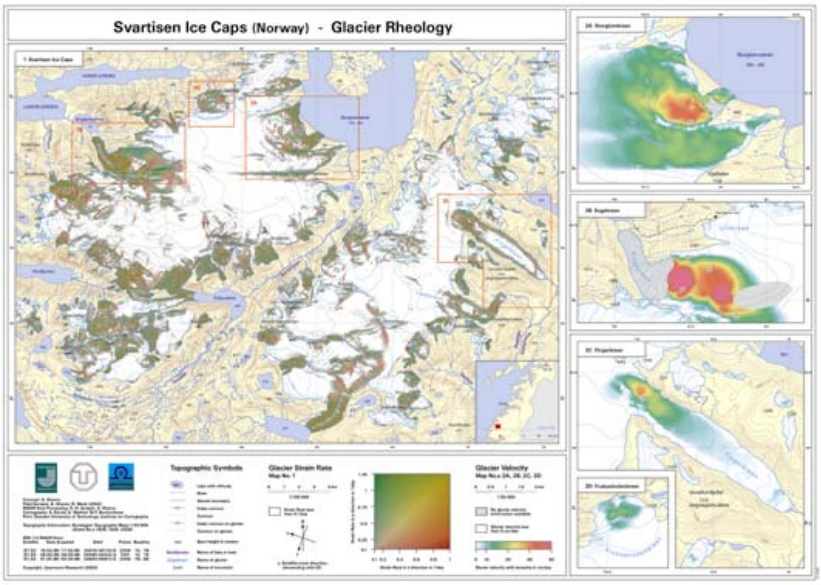

Figure 4. Satellite rheological image map of Svartisen Ice Caps, Northern Norway.

Table 2. GINSAR velocities (cm/day, III-IV 1996) versus average annual velocities in the SV test site

GINSAR veloc-s	31.0	25.0	15.0	14.5	12.0	14.0	12.5	7.0	6.0	5.5	5.5
Photogrammetric	28.0	25.0	17.0	15.0	15.0	13.0	12.5	6.0	6.0	6.0	5.0

The absolute accuracy of determining glacier velocity in the HF test site was evaluated by comparing independent estimates of ice motion from spaceborne interferometric data and from terrestrial surveys by Mr. H.Schneider. Average horizontal velocities at 32 (from 34) stakes installed on the surface of Hintereisferner Glacier at altitudes ranging from 2560 to 2920 m a.s.l. and corresponding velocities obtained by the GINSAR and conventional 2-pass DINSAR techniques are graphically shown in Figure 5. For this site/season, the mean value of reference function *a(x,y)* was close to 0.98.

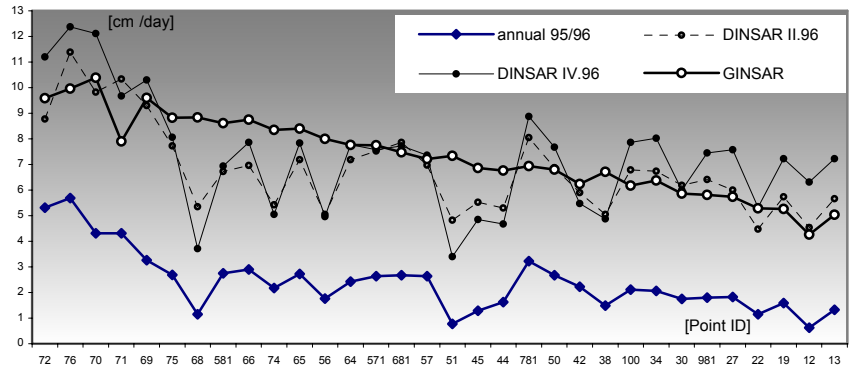

Figure 5. GINSAR and 2-pass DINSAR velocities (cm/day, II-IV 1996, non-calibrated) versus average annual velocities 1995/96 on Hintereisferner Glacier, Austrian Alps

The glacier velocities surveyed in the field were generally consistent with both the GINSAR and 2-pass DINSAR values, although the GINSAR values were far less scattered. One can see, however, that there is a systematic difference of about +5.0 cm/day between the interferometric velocities and those from field surveys. The procedure of calibration and linear adjustment applied to the GINSAR model reduced the mean difference between interferometric and field velocities to +0.2 cm/day and resulted in an estimated r.m.s. difference of ± 1.8 cm/day.

The short-term frontal velocities of 4 test tidewater glaciers (Mack, Rozhdestvenskogo, Rykachova and Shokal'skogo) surveyed in the field in summer 2001 were significantly higher (196% in average) than the velocities measured in the lab from winter interferograms, which was explained by seasonal changes in the glacier flow. Indeed, the speed of glacial flow increases notably in the melt season with the most intense precipitation, and for many tidewater glaciers in the WeRA the summer motion rate is about twice as high as that in the coldest month [13]. Nevertheless, the spatial correlation between the interferometric winter velocities and short-term summer velocities from field surveys was quite high for all 22 target points in the WeRA.

Conclusions

All in all, we can conclude that the phase gradient approach to modelling glacier dynamics based on simple deterministic procedures ensures serious processing advantages, yet without compromising on accuracy. The average tachometric accuracy of the GINSAR technique is about ± 2.0 cm/day. High metric quality and detail, attractive appearance and complementary information contents of the value-added GINSAR products, such as topograms, fluxograms, velograms and slope maps, show the expedience of this technique and its applicability to rheological modelling in different glacier environments.

Acknowledgements

The ERS-1/2-INSAR data for our studies were generously provided by ESA.

References

1. I. Joughin *et al*., "Estimation of ice-sheet motion using satellite radar interferometry". *J.Glac.,* **42** (142), 564-575 (1996).
2. R.Goldstein, R.Engelhard, B.Kamb, and R.Frolich, "Satellite radar interferometry for monitoring ice sheet motion: application to an Antarctic ice stream". *Science*, **262**, 1525-1530 (1993).
3. I.Joughin, R.Kwok, and M.Fahnestock, "Interferometric estimation of three-dimensional ice-flow using ascending and descending passes". *IEEE Trans. Geosc. &RS*, **36** (1), 25-37 (1998).
4. R.Forster *et al.*, "Interferometric radar observations of Glaciers Europe and Penguin". *J.Glac.,* **45** (150), 325-336 (1999).
5. J. Dowdeswell *et al.,* "Velocity structure, flow instability and mass flux on a large Arctic ice cap from satellite radar interferometry". *Earth and Planetary Sc. Letters*, **167**, 131-140 (1999).
6. T.Murray *et al.,* "Ice dynamics during a surge of Sortebræ, East Greenland". *Annals of Glaciology*, **34**, 323-329 (2002).
7. Webster's New Encyclopaedic Dictionary. Black Dog & Leventhal Publishers, New York, 1639 p. (1996).
8. D.R.Fatland and G.Lingle, "Analysis of the 1993-95 Bering Glacier surge using differential SAR interferometry". *J.Glac.,* **44** (148), 532-545 (1998).
9. B.T.Rabus and D.R.Fatland, "Comparison of SAR-interferometric and surveyed velocities on a mountain glacier: Black Rapids Glacier". *J. Glac.,* **46** (152), 119-128 (2000).
10. T.Nagler, C.Mayer and H.Rott, "Feasibility of DINSAR for mapping complex motion fields of Alpine ice- and rock-glaciers". *ESA SP-475*, 377-382 (2002).
11. B.Kjöllmoen (Ed.), "Glaciological investigations in Norway in 2001". NVE Report **1**, 102 p. (2003).
12. M.Kuhn *et al.,* "Measurements and models of the mass balance of Hintereisferner". *Geografiska Annaler*, **81A**, 4, 659-670, 1999.
13. V.S.Koryakin, "Glaciers of the Arctic". Nauka, Moscow, 159 p. (1988, in Russian).
14. C.L.Werner *et al*., "Techniques and applications of SAR interferometry for ERS-1 topographic mapping, change detection, and slope measurement". *ESA SP-359*, 205-210 (1993).
15. U.Wegmüller, C.L.Werner and P.A.Rosen, "Derivation of terrain slopes from SAR interferometric phase gradient". *ESA-SP361*, 711-715 (1994).
16. D.Sandwell and E.Price, "Phase gradient approach to stacking interferograms". *J. Geophys. Res*., **103**, **B12**, 30183-30204, 1998.
17. A.I.Sharov, K.Gutjahr, F.Meyer and M.Schardt, "Methodical alternatives to the glacier motion measurement from differential SAR interferometry". *IAPRS*, **XXXIV**, **3A**, 324 – 329 (2002).